Heats of Formation of the Acetyl Radical and Ion Obtained by Threshold Photoelectron Photoion Coincidence

Elizabeth A. Fogleman, Hideya Koizumi, James P. Kercher, Bálint Sztáray,† and Tomas Baer*

Department of Chemistry, University of North Carolina, Chapel Hill, North Carolina 27599-3290

Received: February 10, 2004; In Final Form: April 12, 2004

The dissociative photoionization onsets for the production of $CH_3CO^+ + CH_3^\bullet$ from acetone and $CH_3CO^+ + CH_3CO^\bullet$ from butanedione have been measured by threshold photoelectron photoion coincidence (TPEPICO) in which time-of-flight (TOF) mass spectra are obtained as a function of the ion internal energy. The use of velocity focusing for threshold electrons and the subtraction of "hot" electron coincidences from the TPEPICO spectra allow the 0 K dissociation onset to be measured with a precision of 1 kJ/mol. The experimental onset for $CH_3^\bullet$ loss from CH_3COCH_3 was measured to be 10.563 ± 0.010 eV and the onset for $CH_3CO^\bullet$ loss from $CH_3COCOCH_3$ was found to be 10.090 ± 0.006 eV. A 298 K heat of formation of the CH_3CO^+ of 659.4 ± 1.1 kJ/mol is obtained by combining the measured dissociation onset with the well-established heats of formation of acetone and the methyl radical. A 298 K heat of formation of the $CH_3CO^\bullet$ radical of −9.8 ± 1.8 kJ/mol is obtained by combining the measured dissociation onset with the well-known heat of formation of butanedione and the measured heat of formation of CH_3CO^+. The acetone and butanedione ionization energies were measured to be 9.708 ± 0.004 and 9.21 ± 0.05 eV, respectively.

Introduction

The heats of formation of the acetyl radical, $CH_3CO^\bullet$, and its closed shell ion, CH_3CO^+, are important because they are related to a number of important thermochemical quantities, such as the C−H bond energy in acetaldehyde and the C−CH_3 bond energy in acetone. It is thus of some importance to establish these quantities to the same level of accuracy as the heats of formation of the related acetaldehyde and acetone molecules. There are several methods for determining bond energies and radical heats of formation, which have been summarized and compared by Berkowitz et al.[1] and Blanksby and Ellison.[2] Among these are negative and positive ion thermochemical cycles as well as methods based on neutral kinetics. All of these approaches for determining a radical or ion heat of formation depend on the accuracy of other measurements. The various approaches thus differ not only in their experimental techniques, but also in their dependence on ancillary thermochemical information. It is thus important to determine these thermochemical quantities by several methods. In this paper we present new experimental data that serve to establish the heats of formation of the acetyl radical and ion to a precision of less than 2 kJ/mol.

The heat of formation of the acetyl ion can be obtained from proton affinity measurements through the reaction

$$H_2C{=}C{=}O + H^+ \rightarrow CH_3CO^+ \qquad \Delta E = PA(H_2C{=}C{=}O)$$

The gas-phase proton affinity is generally measured as a relative quantity by equilibrium methods in high-pressure mass spectrometry, and its accuracy depends on a knowledge of the proton affinity of neighboring molecules in the scale.[3] The 298 K proton affinity of ketene as listed in the NIST webbook is 825.3 kJ/mol,[4] a number that was verified by high-level ab initio calculations of Smith and Radom[5] (825.0 kJ/mol). On the basis of the 0 K value of 819.1 kJ/mol and the heat of formation of ketene and H^+,[6] the 0 K acetyl ion heat of formation is 664.2 ± 4 kJ/mol. The error limits are difficult to determine because they are based on the reliability of the PA scale in the vicinity of ketene. We estimate it to be 4 kJ/mol.

The acetyl ion heat of formation can also be determined from photoionization of a variety of precursor molecules, $CH_3COX + h\nu \rightarrow CH_3CO^+ + X$. Among the factors that determine the best choice are the accuracy of the $\Delta_f H°(CH_3COX)$ and $\Delta_f H°(X)$, the lack of a reverse activation barrier for X loss, and a rapid dissociation reaction that does not involve metastable ions. Finally it is essential that X loss be the lowest energy dissociation channel. Traeger et al.[7] investigated several precursors, which resulted in a broad range of derived acetyl ion heats of formation. Probably the most reliable precursor is acetone, which had a reported 298 K onset of 10.38 eV. A subsequent evaluation of this onset that takes into account the molecule's thermal energy resulted in a reported $\Delta_f H_{298}(CH_3CO^+)$ of 654.7 ± 1.5 kJ/mol.[8] However, an earlier photoionization study by Murad and Inghram[9] had suggested an onset of 10.45 eV, while a more recent study by Trott et al.[10] using a supersonically cooled jet reported an onset of 10.52 eV. One of the problems with photoionization studies is the interpretation of the onset. Because the sample usually has a room temperature thermal energy distribution, the onset must be carefully modeled by taking this into account, as suggested by Asher et al.[11] This was not done in the previous photoionization studies.

The main information about the $CH_3CO^\bullet$ radical heat of formation has come from neutral kinetic methods. Niiranen et al.[12] investigated the forward and backward rate constants for the reaction $CH_3CO^\bullet + HBr \leftrightarrow CH_3CHO + Br^\bullet$ as a function of temperature. Knowing the heat of formation of acetaldehyde, HBr, and the bromine atom permitted them to extract a 298 K

* Corresponding author. E-mail: baer@unc.edu.

† Current address: Department of General and Inorganic Chemistry, Eötvös University Budapest, Hungary H-1117, Budapest, Pázmány P. sétány 1/a.

10.1021/jp040118s CCC: $27.50
Published on Web 05/22/2004

acetyl radical heat of formation of -10.0 ± 1.2 kJ/mol. A subsequent critical review of various kinetic methods led Tsang[13] to propose a 298 K heat of formation of the acetyl radical of -12.0 ± 3 kJ/mol.

In principle, the acetyl free radical heat of formation can be determined through a positive ion cycle. If the acetyl ion heat of formation is known, the radical ionization energy would provide a measure of the radical heat of formation. However, the $CH_3CO^{\bullet}$ ionization energy has not been determined and would be rather difficult to measure with great precision unless it was done with a very cold sample and at very high resolution so that the adiabatic ionization energy could be extracted.

In the negative ion cycle, the gas-phase acidity of CH_3CHO is combined with the $CH_3CO^{\bullet}$ electron affinity:

$$CH_3CHO \rightarrow CH_3CO^- + H^+ \qquad \Delta E = \Delta_{acid}H°(CH_3CHO)$$

$$CH_3CO^{\bullet} + e^- \rightarrow CH_3CO^- \qquad \Delta E = -EA(CH_3CO^{\bullet})$$

When these two reactions are combined with the ionization energy of the hydrogen atom, we obtain the acetaldehyde C−H bond energy: $CH_3CHO \rightarrow CH_3CO^{\bullet} + H^{\bullet}$, which is given by $\Delta_{acid}H°(CH_3CHO) + EA(A^{\bullet}) - IE(H^{\bullet})$. An acetaldehyde gas-phase acidity of $1{,}632 \pm 8$ kJ/mol was estimated by DePuy et al.[14] in a flowing afterglow instrument. A direct measurement was not reported because the acetyl anion is less stable than the isomeric acetaldehyde enolate anion, so that determining this by reaction kinetics was not possible. The electron affinity of the acetyl radical of 0.423 ± 0.038 eV was reported by Nimlos et al.[15] from the CH_3CO^- photoelectron spectrum. Because of the considerable change in the geometry upon electron detachment, the PES consists of a broad band of resolved vibrational peaks in which it is difficult to identify the adiabatic onset from hot bands. Thus the adiabatic EA could be either the published value of 0.423 or 0.481 ± 0.037 eV.[16] Making matters still more uncertain is the heat of formation of aceteldhyde, which Pedley[17] lists as -166.1 ± 0.5 kJ/mol, and Wiberg et al.[18] report as -170.7 ± 1.5 kJ/mol. Thus by combining the various possible values, we can obtain 298 K $CH_3CO^{\bullet}$ heats of formation ranging from -17.2 to -27.9 kJ/mol. These are all considerably lower than the -10.0 kJ/mol value reported by Niiranen et al.[12]

A final route to the acetyl radical heat of formation is through the dissociative photoionization of butanedione, which yields $CH_3CO^+ + CH_3CO^{\bullet}$. If the acetyl ion heat of formation is known, then the radical energy can be determined. Traeger et al.[7] reported the photoionization onset for the acetyl ion to be 9.88 eV, from which Traeger and Kompe[8] determined the 298 K heat of formation of the acetyl radical to be -11.1 ± 1.8 kJ/mol, which is quite close to the value obtained from the neutral kinetic method.

This review of the experimental acetyl ion heat of formation shows that there is considerable disagreement among the reported values of the acetone dissociative photoionization onsets. However, there seems to be sufficient flexibility in their interpretation that the derived CH_3CO^+ heat of formation can be made to agree with the value derived from the ketene proton affinity. In the case of the acetyl radical heat of formation, the kinetic methods yield values that are 12 kJ/mol higher than the value from the negative ion cycle. On the other hand the photoionization and kinetic methods agree quite well.

We present in this paper photoionization data that provide new values for these heats of formation with overall error limits of ± 2 kJ/mol. In this study the dissociative photoionization onsets of acetone to give $CH_3CO^+ + CH_3$ and butanedione to yield $CH_3CO^+ + CH_3CO^{\bullet}$ are used to establish the acetyl ion and radical heats of formation. The experimental development that has made such a precision in determining the dissociation limits possible is a recently implemented threshold photoelectron photoion coincidence experiment that is free from the contribution of energetic electrons, and thus provides an unambiguous and accurate method for determining the 0 K dissociation onset.[19,20]

Experimental Approach

General issues concerning photoelectron photoion coincidence spectroscopy have been described previously,[21] and a method for subtraction of "hot" electrons has also been published.[20] In this section, we describe some improvements implemented since the previous publication. The room temperature sample, introduced through a hypodermic needle into the ionization region, was ionized with vacuum ultraviolet (VUV) light from a H_2 discharge lamp dispersed by a 1 m normal incidence vacuum monochromator. The entrance and exit slits were 100 μm, which yielded a resolution of 1 Å (12 meV at a photon energy of 10 eV). The energies were calibrated by using the hydrogen Lyman-α resonance line at 10.199 eV. A 20 V/cm extraction field was used to accelerate ions and electrons in opposite directions, using velocity focusing optics[22] for electrons, which yields a resolution of 13 meV.[19] Electrons were extracted toward an electrode with a gridless 12.7-mm aperture located 6 mm from the center of the ionization region. A second acceleration electrode (with a gridless 12.7-mm aperture), located 12 mm from the first one, accelerated the electrons to 67 V. The electrons then drifted approximately 13 cm through a field free flight tube, which was terminated by an aperture containing a central 1.5-mm hole and an opening in the shape of a ring with inner and out diameters of 6 and 10 mm. The electrons were detected by either a Burle channeltron (located behind a 1.5-mm aperture situated on the extraction axis) or a Burle multichannel plate (MCP), which collected electrons that passed through the ring around the central hole. The MCP had a 5-mm hole in the center to permit the channeltron to collect the central electrons. The use of two separate detectors, rather than a single MCP, eliminated cross talk between the two signals.

Velocity-focused electrons with zero kinetic energy passed through the central aperture and were detected by the channeltron. In addition, energetic electrons, whose initial velocities were in a direction parallel to the extraction voltage, were also detected by the channeltron. This is the source of the "hot electron" contamination that has plagued TPEPICO experiments in the past.[23,24] Energetic electrons whose initial velocities were perpendicular to the extraction axis were focused onto concentric rings around the central spot, the radii being proportional to the initial velocity perpendicular to the extraction axis. Assuming that the hot electron ring signal is proportional to the hot electron contribution in the center, a weighted fraction of the ring signal could be subtracted from the central signal and thus correct the threshold electron signal.[20] It is thus possible to collect threshold photoelectron spectra (TPES) and threshold photoelectron photoion coincidence (TPEPICO) free of hot electrons.

The ions were accelerated over a 5-cm region before drifting 40 cm through the first field free drift region to a single stage 40 cm long reflectron, where they were decelerated and reflected. After exiting the reflectron, the ions drift approximately 40 cm through the second field free drift region before being detected on tandem Burle MCPs. The electrons and ions gave the start and stop signals for the TOF measure-

ments, respectively, and the coincidence events were stored on multichannel pulse height analyzers. Since both ring and center electrons were used as start signals two TOF measurements were simultaneously recorded at each photon energy. The TOF measurements were recorded for 1−24 h, depending on the signal intensity and desired spectrum quality. The collection efficiency for threshold electrons was about 30% and that of ions about 7%.

The integrated TOF peaks were then used to calculate breakdown diagrams for the central and the ring TOF spectra. The breakdown diagram is the fractional abundance of parent and fragment ions as a function of the photon energy. For instance, the fractional abundance of the parent ion for the central electrode is $B(P_c) = P_c/T_c$, where P_c and T_c are the integrated ion signals for the parent and total ions associated with the central electrode, respectively. A similar breakdown can be constructed for the ring electrode. The hot electron contribution was then subtracted by the following equation:

$$B(P) = \frac{B(P_c) - fB(P_r)}{1 - f} \quad (1)$$

where f is a constant factor and the $1 - f$ in the denominator normalizes the B function.

Threshold photoelectron spectra (TPES) were recorded for acetone and butanedione as well. The monochromator was scanned at a rate of 0.5 A/min while electron signals were collected from the central (channeltron) and ring (multichannel plate) detectors for 12 s/point. These two electron signals were then normalized by dividing the signal by the photon intensity. As in the coincidence experiments, a hot electron contamination is present in the threshold signal. To correct for this, the ring signal was subtracted from the central spectrum and the true threshold photoelectron spectrum is obtained as in eq 2,

$$I_{thres} = I_c - fI_r \quad (2)$$

where I_{thres} is the true threshold photoelectron intensity, I_c is the center normalized signal intensity, and I_r is that for the ring. The factor f was held constant over this energy range.

Acetone and butanedione were purchased from Sigma Aldrich and were used without further purification.

Results

Threshold Photoelectron Spectra. Threshold photoelectron spectra (TPES) of our two molecules were collected to determine in which region of the photoelectron spectrum the ions dissociated. Figure 1 shows the TPES for acetone. The ring and center electrode signals are plotted as dots and a gray line, respectively. The subtracted spectrum, which represents the true TPES, is shown as the heavy solid line. The width of the first peak of 17 meV is nearly limited by the resolution of our instrument (13 meV). The factor by which the center electrode signal was multiplied before data subtraction was determined by collecting a TPEPICO TOF spectrum at an energy of about 11 eV, well above the dissociation limit for CH_3 loss. At this energy, all parent ion signal in the center spectrum is the result of hot electrons. Thus the factor can be set equal to the ratio of parent ion signal in the ring and central electrode TOF distributions, which is 0.278. The ionization energy of 9.708 ± 0.004 eV agrees perfectly with the most accurate measurement of the acetone ionization energy obtained in a ZEKE/PFI study of Wiedmann et al.,[25] who reported an IE of 9.7080 ± 0.0001 eV. This IE is slightly higher than the 9.703 ± 0.006 eV value listed in the NIST database,[26] and 12 meV higher than the 9.696 ± 0.006 eV reported by Trott et al.[10] on the basis of their molecular beam photoionization study. It is evident that the yield of threshold electrons in the Franck−Condon gap region beyond about 10 eV is very weak, and that most of the center electrode signal is a result of hot electrons. This makes determination of the dissociation onset, which lies in this region, challenging. Indeed, Traeger pointed out the very weak CH_3CO^+ signal in the vicinity of its appearance energy.[7,8]

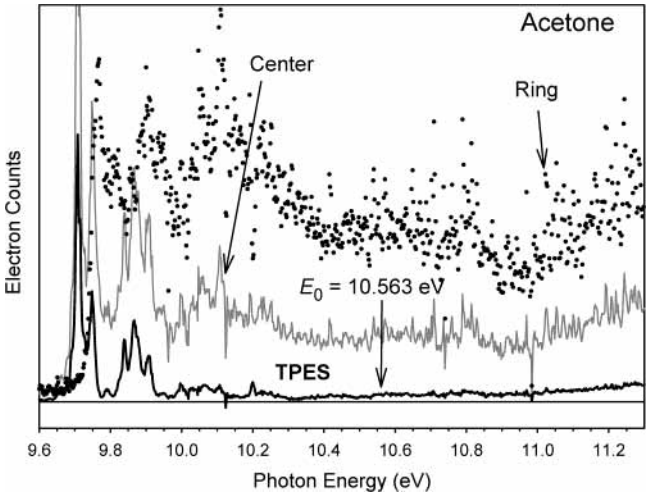

Figure 1. The threshold photoelectron spectrum (TPES) of acetone in the vicinity of its ionization energy. The center signal collects both threshold electrons and some "hot" electrons, whereas the ring signal collects only hot electrons. The subtracted signal (dark line) is the true TPES. The E_0 indicates the dissociation limit for $CH_3^\bullet$ loss.

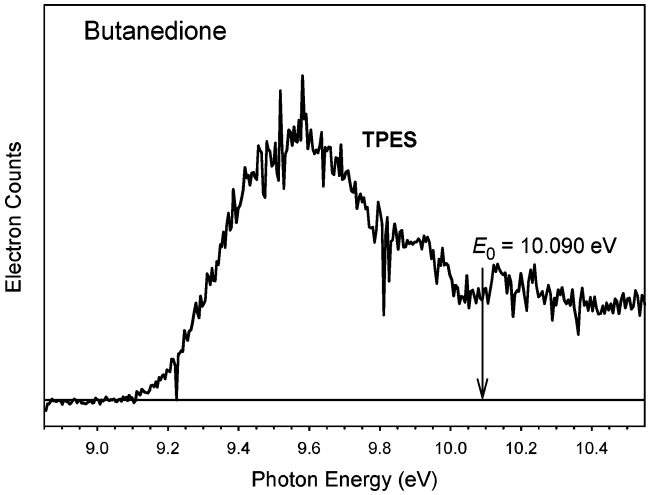

Figure 2. The TPES for butanedione in the vicinity of its ionization energy. The E_0 indicates the dissociation limit for the loss of $CH_3CO^\bullet$.

The corrected TPES of butanedione is shown in Figure 2. This spectrum differs from the acetone TPES in the very broad first band, which is indicative of a large change in geometry upon ionization. Indeed our ab initio calculations show that the middle C−C bond distance changes from 1.557 to 1.981 Å upon ionization. The determination of the adiabatic ionization energy is difficult, and we estimate it to be 9.21±0.05 eV, which is somewhat lower than the values reported by Watanabe et al.[27] (9.23 eV) or Traeger et al.[7] (9.3 eV). The broad peak extends to an energy beyond the derived fragmentation onset, so that the yield of threshold electrons is significant in this critical region.

TPEPICO TOF Spectra and Breakdown Diagrams. *Acetone.* TOF mass spectra of acetone were collected in the photon energy range from 10.16 to 10.83 eV. In this region, the parent

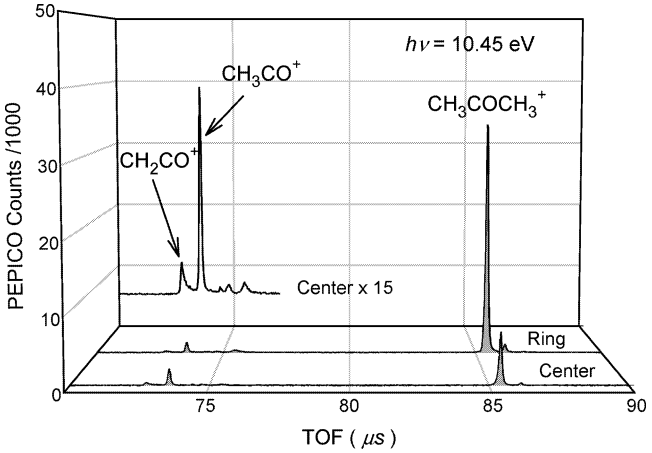

Figure 3. The TPEPICO time-of-flight distribution for acetone at 10.45 eV. The CH_2CO^+ peak is slightly asymmetric, characteristic of a slow dissociation, whereas the CH_3CO^+ peak is symmetric. The other three peaks at around 75 μs are due to the ^{13}C peak contribution, a metastable peak for CH_2CO^+ formed in the drift tube of the reflectron, and a collision-induced dissociation peak.

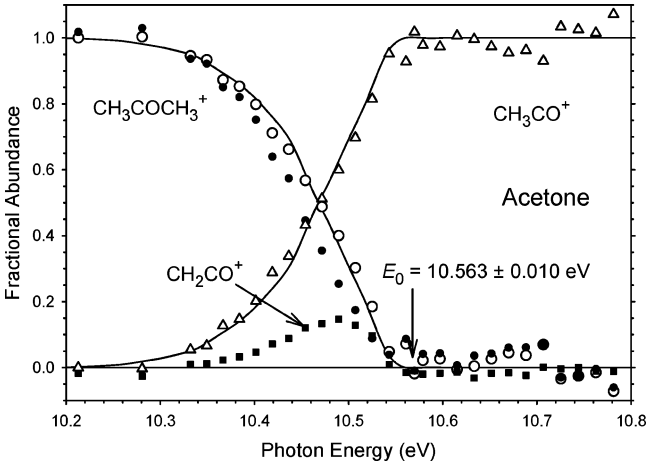

Figure 4. The experimental breakdown diagram for the acetone ion (points). The solid circles are the parent ion and the solid squares are the CH_2CO^+ data. When these are added together, they yield the open circles (see text for explanation). The open triangles are the CH_3CO^+ points. These data have been corrected for "hot" electron contributions as explained in the text. The solid lines constitute the calculated breakdown diagram at 298 K in which the only adjustable parameter is the 0 K dissociation limit, indicated by the vertical arrow.

ion, $CH_3COCH_3^+$, and two fragment ions, CH_3CO^+ and CH_2CO^+, are observed. The latter is a minor fragment associated with a rearrangement that results in the loss of CH_4. The TOF distribution taken at a photon energy of 10.45 eV is shown in Figure 1. The center signal is expanded by a factor of 15 in the inset and shows the narrow and symmetric CH_3 loss fragment peak as well as the slightly asymmetric CH_4 loss fragment peak. The asymmetric peak indicates that the production of ketene ion proceeds via a long-lived or metastable parent ion. A very slow component that corresponds to dissociation in the first drift region before the reflectron shows up as a peak around 76 μs. The other two small peaks are a result of the ^{13}C isotope and a collision-induced dissociation in the drift region of the reflectron. The mechanism for this slow reaction for CH_4 loss has been of considerable interest.[28,29] A low-energy enol ion isomer is certainly involved but a tunneling step associated with the proton transfer may also intervene. Although we could measure the dissociation rate as a function of the ion energy, we choose not to focus on this issue in this study. Rather we simply note that the CH_4 reaction has an onset below that of the CH_3 loss, and because it is slow, we assume that once the CH_3 loss step is energetically accessible, it will dominate the reaction. The $CH_3^\bullet$ loss reaction producing the CH_3CO^+ ion results in a symmetric acetyl ion TOF peak, which indicates that it is produced by a fast reaction.

By collecting TOF spectra at various photon (ion internal) energies, and plotting the relative abundance of parent and daughter ions, we obtain the breakdown curve for acetone as shown in Figure 4. This breakdown diagram has been corrected for hot electrons as described in the Experimental Section. At low energies, the parent ion has insufficient energy to dissociate so that its fractional abundance is 1. At the same time, the fractional abundance of the CH_3CO^+ ion rises from 0 to 1 at high energies. We also see the CH_4 loss channel rise and decrease between 10.4 and 10.55 eV. However, the CH_2CO^+ signal disappears at the 0 K threshold for the acetyl ion, which shows that when the ion has sufficient energy to produce the acetyl ions, it will do so and will not dissociate via methane loss. The open circles are the combined parent and ketene ion signals, which are summed to determine the onset for the acetyl ion.

The solid lines are the calculated breakdown diagram in which the neutral acetone sample internal energy distribution, P(E), is taken into account. All ions that have an energy in excess of the 0 K dissociation limit, E_0, are assumed to dissociate immediately. Because the ion internal energy is a sum of the photon energy plus the neutral internal energy, the parent and daughter ion curves are given by

$$B_P(h\nu) = \int_0^{E_0-h\nu} P(E)\,dE \qquad \text{for } h\nu < E_0 \quad (B_P(h\nu) = 0 \text{ for } h\nu > E_0) \quad (3)$$

$$B_D(h\nu) = \int_{E_0-h\nu}^{\infty} P(E)\,dE \qquad \text{for } h\nu < E_0 \quad (B_D(h\nu) = 1 \text{ for } h\nu > E_0) \quad (4)$$

The thermal ro-vibrational energy distribution was calculated by using both the experimental acetone vibrational frequencies taken form Shimanouchi[30] and frequencies calculated at the B3LYP/6-311++G** level of theory with the G98 Gaussian package.[31] The experimental and unscaled calculated frequencies for the acetone molecule, shown in Table 1, generally agreed to within 5%. More importantly, the average thermal energy calculated with these two sets of frequencies agreed to within 0.1 kJ/mol. This confirms a finding by Magalhaes and Soares Pinto,[32] who found that B3LYP/6-311++G** frequencies should not be scaled.

The best fit of the experimental breakdown curve, shown in Figure 4, is obtained when the 0 K dissociation limit, E_0, is set at 10.563 ± 0.010 eV. The model reproduces the experimental breakdown curve well over the entire energy range studied. The derived E_0 for this reaction is slightly higher than the 10.52 ± 0.01 eV reported by Trott et al.[10] on the basis of a molecular beam photoionization study. In that study, the onset was determined by extrapolating the CH_3CO^+ signal as a function of the photon energy to the baseline. They also assumed that the molecule was at 0 K. However, if the cooling is not complete, the onset would shift toward lower energy. The authors were aware of this and suggested that the E_0 is likely to be 10.54 eV or higher. It is worth noting that the calculated breakdown diagram using calculated frequencies at the B3LYP/6-311++G** level of theory is identical to the breakdown diagram using experimental frequencies.

TABLE 1: Calculated Vibrational Frequencies[a]

acetone neutral	68, 133, 380, 490, 536, 782, 884, 889, 1083, 1116, 1232, 1386, 1387, 1461, 1465, 1472, 1488, 1786, 3024, 3031, 3079, 3086, 3139, 3140
acetone ion	75, 134, 335, 367, 475. 688, 893, 899, 1001, 1060, 1073, 1299, 1343, 1419, 1423, 1440, 1459, 1625,3025, 3031, 3104, 3110, 3177, 3178
butanedione neutral	39, 103, 106, 238, 348, 360, 519, 546, 617, 682, 910, 956, 1012, 1065, 1133, 1272, 1386, 1392, 1456,1456, 1458, 1461, 1782, 1783, 3041, 3041, 3097, 3097, 3149, 3149
butanedione ion	11, 92, 99, 195, 200, 303, 340, 466, 482, 511, 882, 895, 1002, 1028, 1038, 1041, 1363, 1368, 1423, 1428,1439, 1440, 2003, 2009, 3039, 3039, 3114, 3115, 3145, 3147
acetyl radical	110, 469, 855, 956, 1049, 1358, 1453, 1457, 1925, 3016, 3108, 3114
acetyl ion	418, 419, 910, 1028, 1028, 1363, 1396, 1396, 2385, 2999, 3080, 3081
methyl radical	537, 1402, 1402, 3102, 3282, 3282

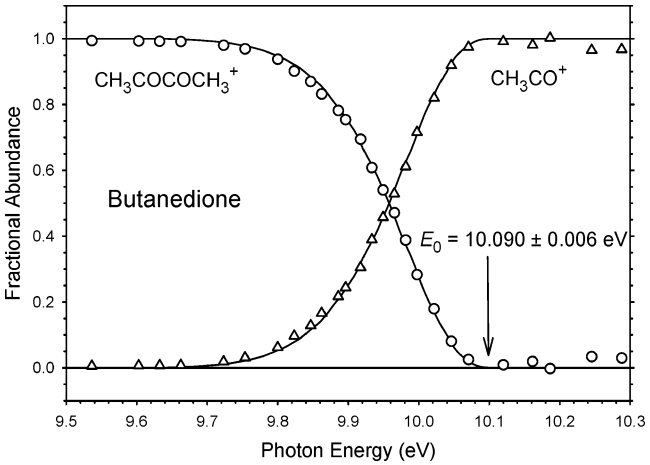

Figure 5. The experimental breakdown diagram for butanedione (points). The solid lines constitute the calculated breakdown diagram in which the only adjustable parameter is the 0 K dissociation limit indicated by the vertical arrow.

Figure 5 shows the breakdown diagram for butanedione, in which the only fragment observed was the acetyl ion. Because no experimental vibrational frequencies are available for this molecule, we calculated the breakdown diagram for a temperature of 298 K using the butanedione vibrational frequencies (Table 1) calculated with the B3LYP/6-311++G** level of theory in the G98 Gaussian package.[31] When we use our derived ionization energy of 9.21 eV, the best fit to the experimental breakdown diagram is with an $E_0 = 10.090 \pm 0.006$ eV. The value of the ionization energy is important here because this molecule, which is larger than acetone, has a sufficiently large density of vibrational states that the calculated RRKM rate constant at threshold is about 10^3 s^{-1}. The asymmetry of the acetyl ion TOF peak confirms this slow rate. As a result, the observed E_0 is shifted to higher energies by about 10 meV, and the modeling of the breakdown diagram takes into account this slow reaction. Had it not been included, the onset would have been 10.101 eV.

The excellent agreement between the experimental and the calculated 298 K breakdown diagram modeled by eqs 3 and 4 justifies the assumption that the ionization process simply transposes the neutral thermal energy distribution into the ion manifold. The validity of this model is fortunate because it means that we are not forced to calculate complicated Franck−Condon factors for each transition connecting ro-vibrational states in the molecule and ion. The excellent fit with the simple theory appears to suggest that the Franck−Condon factors are the same for all transitions independent of the initial neutral molecule vibrational state. Although this is certainly not correct for individual transitions, it appears to be correct when averaged over the thousands of transitions that are involved. While this model works for 298 K TPEPICO experiments, it does not seem to work for cooled samples studied by pulsed field ionization (PFI) PEPICO.[33−35] In those experiments, the pulsed field ionization process seems to favor the product ion channel so that the breakdown diagram cannot be fit by the use of eqs 3 and 4.

TABLE 2: Ancillary Heats of Formation (kJ/mol)

	$\Delta_f H°_{0K}$	$\Delta_f H°_{298K}$	$H°_{298K} - H°_{0K}$[a]
CH_3COCH_3	-202.2 ± 0.6[a]	-218.5 ± 0.6[b]	16.6
$CH_3COCOCH_3$	-310.4 ± 1.2[a]	-327.1 ± 1.2[c]	21.6
$CH_3^•$	150.3 ± 0.4[d]	147.1 ± 0.4[a]	10.5
$CH_3COCH_3^+$	734.5 ± 0.7[e]	718.8 ± 0.7[e]	17.2
$CH_3COCOCH_3^+$	578.2 ± 5.0[f]	563.8 ± 5.0[f]	23.9
CH_4	-66.4 ± 0.4	-74.4 ± 0.4[c]	9.99
$H^•$	216.0[g]	218.0[g]	6.12[g]

[a] Conversion calculated by using experimental or ab initio vibrational frequencies from Table 1. [b] From Wiberg et al.[18] [c] From Pedley.[17] [d] Determined from $\Delta_f H_{0K}(CH_3^+)$ from Weitzel et al.[34] and $IE(CH_3^•)$ from Blush et al.[36] [e] Ionization energy of CH_3COCH_3 from this study. [f] Ionization energy of $CH_3COCOCH_3$ from this study. [g] From Wagman et al. [6]

CH_3CO^+ and $CH_3CO^•$ Thermochemistry. The measured 0 K dissociation limits obtained from the breakdown diagrams permit us to derive values for the heats of formation of the acetyl ion and free radical. The 0 K heat of formation of the acetyl ion is given by

$$\Delta_f H°_{0K}[CH_3CO^+] = E_0 + \Delta_f H°_{0K}[CH_3COCH_3] - \Delta_f H°_{0K}[CH_3^•] \quad (5)$$

The 298 K heat of formation of acetone is listed in Pedley[17] as -217.1 ± 0.7 kJ/mol. However, this compilation did not include the work of Wiberg et al.,[18] who measured the heats of formation of a number of carbonyl compounds relative to their alcohol counterparts. They list a value of -218.5 ± 0.6 kJ/mol. This number can be transformed to a 0 K value by the usual thermochemical cycle, using the experimental values for the acetone vibrational frequencies and the known $H°_{298K} - H°_{0K}$ values for the elements as listed in Wagman et al.[6] The transformation, which is given by

$$\Delta_f H°_{0K} = \Delta_f H°_{298K} + \sum(H°_{298K} - H°_{0K})_{elements} - (H°_{298K} - H°_{0K})_{molecule} \quad (6)$$

yields $\Delta_f H°_{0K}[CH_3COCH_3] = -202.2 \pm 0.6$ kJ/mol. These values along with other ancillary heats of formation are listed in Table 2. The methyl radical heat of formation is known very accurately as a result of the recently measured 0 K onset for the $CH_4 + h\nu \rightarrow CH_3^+ + H^•$ reaction (14.323 ± 0.001 eV).[34] When this is combined with the even more accurate methyl radical ionization energy of 9.8381 ± 0.0001 eV,[36] we obtain $\Delta_f H°_{0K}[CH_3^•] = 150.3 \pm 0.4$ kJ/mol, in which the error is limited by the methane heat of formation. This results in a

TABLE 3: Experimental Measurements of $\Delta_f H°(CH_3CO^+)$ (kJ/mol)

method	measured value	$\Delta_f H°_{0K}$	$\Delta_f H°_{298K}$	$H_{298K} - H_{0K}$
$CH_3COCH_3 + h\nu \rightarrow CH_3CO^+ + CH_3$				
photoionization (PI)[a]	10.45 eV (0 K)			
photoionization[b]	10.38 eV (298 K)		654.7 ± 1.1[c]	
molecular beam PI[d]	10.52 eV (0 K)			
TPEPICO[e]	10.563 eV (0 K)	666.7 ± 1.1	659.4 ± 1.1	11.82
ketene proton affinity	825.3 kJ/mol (298 K)[f]	664.2 ± 2	656.9[g]	12.0[h]
$CH_2CO + H^+ \rightarrow CH_3CO^+$				

[a] This is an extrapolated 0 K value by Murad and Inghram.[9] [b] From Traeger et al.[7] [c] Reevaluation by Traeger and Kompe[8] in which the thermal energy is taken into account. [d] From Trott et al.[10] [e] This work. [f] From Hunter and Lias.[37] [g] Calculated from ketene heat of formation[17] and proton affinity. [h] Calculated by Smith and Radom.[5]

TABLE 4: Experimental Measurements of $\Delta_f H°(CH_3CO^•)$ (kJ/mol)

method	measured value	$\Delta_f H°_{0K}$	$\Delta_f H°_{298K}$	$H_{298K} - H_{0K}$
neutral kinetics				
$CH_3CO^• + HBr \leftrightarrow CH_3CHO + Br^•$	k_f and k_r		−10.0 ± 1.2[a]	12.39[a]
critical review			−12 ± 3[b]	
negative ion cycle				
EA(CH_3CO)	0.423 ± 0.037 eV[c]			
acidity (CH_3CHO)	1632 ± 8 kJ/mol[d]		−22.6 ± 8.8	
butanedione photoionization				
298 K $CH_3CO^•$ onset	9.67 eV[e]			
298 K $CH_3CO^•$ onset	9.88 ± 0.011 eV[f]		−11.1 ± 1.8[g]	
0 K $CH_3CO^•$ onset[h]	10.090 ± 0.006 eV	−3.6 ± 1.8	−9.8 ± 1.8	12.86

[a] From Niiranen et al.[12] [b] From Tsang.[13] [c] From Nimlos et al.[15] The EA could also be 0.481 eV (see text).[16] [d] Estimated acidity from DePuy et al.[14] [e] From Murad and Inghram.[38] [f] From Traeger et al.[7] [g] From Traeger and Kompe.[8] [h] This work.

$\Delta_f H°_{0K}[CH_3CO^+]$ of 666.7 ± 1.2 kJ/mol, in which the error is determined mainly by our measured onset. In converting this heat of formation to 298 K using eq 6, we use the NIST Webbook 0 K electron convention in which $(H°_{298K} - H°_{0K})_{electron}$ is taken to be 0. It differs from the other convention used by the NBS compilation.[6] To convert the 0 K convention to the 298 K convention, $2.5RT = 6.2$ kJ/mol must be added to the acetyl ion heat of formation. The acetyl ion vibrational frequencies used for the 0→298 K conversion are listed in Table 1.

The derived acetyl ion heat of formation, which is compared to literature values in Table 3, is certainly the most accurate one based on the dissociative ionization of the acetone molecule because the TPEPICO approach yields directly a 0 K dissociation limit that is easily extracted from the data. This is not the case in simple photoionization studies in which the onset is determined from a vanishing acetyl ion signal. The shape of such photoionization signals can be affected by the temperature as well as the photoelectron spectrum in the vicinity of the onset.

The only other route to the acetyl ion heat of formation is through the previously mentioned proton affinity of the ketene molecule, which yields a 0 K acetyl ion heat of formation of 664.3 ± 4 kJ/mol. This agrees with our value of 666.7 kJ/mol to within 2.4 kJ/mol, which is within the error of the two measurements. Had we used the acetone heat of formation from Pedley, the discrepancy would have been 3.8 kJ/mol.

The acetone ion C−C bond energy can be determined from the difference in our acetone ionization energy of 9.708 ± 0.004 eV and E_0 of 10.563 ± 0.010 eV. This yields a $CH_3CO^+-CH_3$ bond energy of 0.855 ± 0.010 eV or 82.5 ± 1.0 kJ/mol.

Using the above acetyl ion heat of formation from the acetone experiment in combination with results from the photoionization of butanedione gives a 0 K heat of formation of the acetyl radical. The breakdown diagram of the fragmentation of butanedione to the acetyl radical and acetyl ion was fit with an E_0 of 10.090 ± 0.006 eV. Using this E_0 and the 298 → 0 K converted literature value for $\Delta_f H°_{0K}(CH_3COCOCH_3) = -310.4$ ± 1.2 kJ/mol,[17] the 0 K heat of formation of the acetyl radical can be determined from

$$\Delta_f H°_{0K}(CH_3CO^•) = E_0(CH_3CO^+) + \Delta_f H°_{0K}(CH_3COCOCH_3) - \Delta_f H°_{0K}(CH_3CO^+) \quad (7)$$

which yields $\Delta_f H°_{0K}(CH_3CO^•) = -3.6 \pm 1.8$ kJ/mol. The conversion to 298 K gives $\Delta_f H°_{298K}(CH_3CO^•) = -9.8 \pm 1.8$ kJ/mol. The error of 1.8 kJ/mol represents the sum of our appearance energy (±1 kJ/mol) and the uncertainty in the other heats of formation. The acetyl radical heat of formation, obtained through our ion cycle and shown in Table 4, agrees remarkably well with the values obtained from neutral kinetic measurements, especially the one by Niiranen et al.[12] of −10.0 ± 1.2 kJ/mol. It is interesting, though, that in their calculation of the acetyl radical heat of formation they used $\Delta_f H°_{298K}[CH_3CHO] = -165.8$ kJ/mol, which differs significantly from the Wiberg measured value of −170.7 ± 1.5 kJ/mol.[18] If we were to use the Wiberg heat of formation, the derived Niiranen acetyl radical heat of formation would be −14.9 kJ/mol.

As already pointed out in the Introduction, the negative ion cycle is not a good route for determining the acetyl radical heat of formation because of problems with both the electron affinity and the acetaldehyde acidity determinations.

Conclusions

The heats of formation of the acetyl ion and radical have been measured by dissociative photoionization of acetone and butanedione. The present determination of the 0 K acetyl ion dissociation limit from acetone by threshold photoelectron photoion coincidence (TPEPICO) is more reliable than previous photoionization measurements because the 0 K onset can be unambiguously established. The derived acetyl ion heat of formation agrees to within 2 kJ/mol with a measurement based on the proton affinity of ketene. The good agreement between these different methods lends support for this value and its error limit.

The acetyl radical has been measured by three methods, neutral kinetics, the negative ion cycle, and the dissociation of butanedione, to yield $CH_3CO^{\bullet}$. The neutral kinetics and our TPEPICO onset for the radical from butanedione agree to within 2 kJ/mol. The negative ion cycle in which the gas-phase acidity of acetaldehyde is combined with the radical electron affinity is not a reliable path for determining the acetyl radical heat of formation. This is because the substantial geometry change upon ionization makes determination of the adiabatic ionization energy of CH_3CO^- difficult, and because the heterolytic bond dissociation of acetaldehyde removes the proton from the CH_3 group rather than the CHO group to produce the acetaldehyde enolate ion rather than the acetyl anion.

Acknowledgment. We thank the U.S. Department of Energy for support of this work.

References and Notes

(1) Berkowitz, J.; Ellison, G. B.; Gutman, D. *J. Phys. Chem.* **1994**, *98*, 2744.

(2) Blanksby, S. J.; Ellison, G. B. *Acc. Chem. Res.* **2003**, *36*, 255.

(3) Szulejko, J. E.; McMahon, T. B. *J. Am. Chem. Soc.* **1993**, *115*, 7839.

(4) Hunter, E. P.; Lias, S. G. *Proton Affinity Evaluations in NIST Chemistry WebBook*: *NIST Standard Reference Databas 69*; National Institute of Standards and Technology (http://webbook.nist.gov): Gaithersburg, MD, 1998.

(5) Smith, B. J.; Radom, L. *J. Am. Chem. Soc.* **1993**, *115*, 4885.

(6) Wagman, D. D.; Evans, W. H. E.; Parker, V. B.; Schum, R. H.; Halow, I.; Mailey, S. M.; Churney, K. L.; Nuttall, R. L. The NBS Tables of Chemical Thermodynamic Properties. *J. Phys. Chem. Ref. Data Suppl. 2* 1982, *11*.

(7) Traeger, J. C.; McLoughlin, R. G.; Nicholson, A. J. C. *J. Am. Chem. Soc.* **1982**, *104*, 5318.

(8) Traeger, J. C.; Kompe, B. M. Thermochemical data for free radicals from studies of ions. In *Energetics of Organic Free Radicals*; Martinho Simões, J. A., Greenberg, A., Liebman, J. F., Eds.; Chapman & Hall: London, UK, 1996; pp 59−109.

(9) Murad, E.; Inghram, M. G. *J. Chem. Phys.* **1964**, *40*, 3263.

(10) Trott, W. M.; Blais, N. C.; Walters, E. A. *J. Chem. Phys.* **1978**, *69*, 3150.

(11) Asher, R. L.; Appelman, E. H.; Ruscic, B. *J. Chem. Phys.* **1996**, *105*, 9781.

(12) Niiranen, J. T.; Gutman, D.; Krasnoperov, L. N. *J. Phys. Chem.* **1992**, *96*, 5881.

(13) Tsang, W. Heats of Formation of Organic Free Radicals by Kinetic Methods. In *Energetics of Organic Free Radicals*; Martinho Simões, J. A., Greenberg, A., Liebman, J. F., Eds.; Chapman & Hall: London, UK, 1996; pp 22−58.

(14) DePuy, C. H.; Bierbaum, V. M.; Damrauer, R.; Soderquist, J. A. *J. Am. Chem. Soc.* **1985**, *107*, 3385.

(15) Nimlos, M. R.; Soderquist, J. A.; Ellison, G. B. *J. Am. Chem. Soc.* **1989**, *111*, 7675.

(16) Ellison, G. B.; Bierbaum, V. M., 2004. Personal communication.

(17) Pedley, J. B. *Thermochemical Data and Structures of Organic Compounds*; Thermodynamics Research Center: College Station, TX, 1994.

(18) Wiberg, K. B.; Crocker, L. S.; Morgan, K. M. *J. Am. Chem. Soc.* **1991**, *113*, 3447.

(19) Baer, T.; Li, Y. *Int. J. Mass Spectrom.* **2002**, *219*, 381.

(20) Sztáray, B.; Baer, T. *Rev. Sci. Instrum.* **2003**, *74*, 3763.

(21) Baer, T.; Booze, J. A.; Weitzel, K. M. Photoelectron photoion coincidence studies of ion dissociation dynamics. In *Vacuum ultraviolet photoionization and photodissociation of molecules and clusters*; Ng, C. Y., Ed.; World Scientific: Singapore, 1991; pp 259−298.

(22) Chandler, D. W.; Parker, D. H. *Adv. Photochem.* **1999**, *25*, 59.

(23) Li, Y.; Sztáray, B.; Baer, T. *J. Am. Chem. Soc.* **2001**, *123*, 9388.

(24) Sztáray, B.; Baer, T. *J. Am. Chem. Soc.* **2000**, *122*, 9219.

(25) Wiedmann, R. T.; Goodman, L.; White, M. G. *Chem. Phys. Lett.* **1998**, *293*, 391.

(26) Lias, S. G.; Bartmess, J. E.; Liebman, J. F.; Holmes, J. L.; Levin, R. D.; Mallard, W. G. Ion Energetics Data. In *NIST Chemistry WebBook, NIST Standard Reference Database No. 69*; Mallard, W. G., Linstrom, P. J., Eds.; National Institute of Standards and Technology (http://webbook.nist.gov): Gathersburg, MD, 2000.

(27) Watanabe, K.; Nakayama, T.; Mottl, J. *J. Quant. Spectrosc. Radiat. Transfer* **1962**, *2*, 369.

(28) Heinrich, N.; Louage, F.; Lifshitz, C.; Schwarz, H. *J. Am. Chem. Soc.* **1988**, *110*, 8183.

(29) Nummela, J. A.; Carpenter, B. K. *J. Am. Chem. Soc.* **2002**, *124*, 8512.

(30) Shimanouchi, T. *Tables of Molecular Vibrational Frequencies*; Natl. Stand. Ref. Data. Ser. (NBS) No. 39: U.S. Government Printing Office: Washington, DC, 1972.

(31) Frisch, M. J.; Trucks, G. W.; Schlegel, H. B.; Scuseria, G. E.; Robb, M. A.; Cheeseman, J. R.; Zakrzewski, V. G.; Montgomery, J. A., Jr.; Stratmann, R. E.; Burant, J. C.; Dapprich, S.; Millam, J. M.; Daniels, A. D.; Kudin, K. N.; Strain, M. C.; Farkas, O.; Tomasi, J.; Barone, V.; Cossi, M.; Cammi, R.; Mennucci, B.; Pomelli, C.; Adamo, C.; Clifford, S.; Ochterski, J.; Petersson, G. A.; Ayala, P. Y.; Cui, Q.; Morokuma, K.; Malick, D. K.; Rabuck, A. D.; Raghavachari, K.; Foresman, J. B.; Cioslowski, J.; Ortiz, J. V.; Stefanov, B. B.; Liu, G.; Liashenko, A.; Piskorz, P.; Komaromi, I.; Gomperts, R.; Martin, R. L.; Fox, D. J.; Keith, T.; Al-Laham, M. A.; Peng, C. Y.; Nanayakkara, A.; Gonzalez, C.; Challacombe, M.; Gill, P. M. W.; Johnson, B. G.; Chen, W.; Wong, M. W.; Andres, J. L.; Head-Gordon, M.; Replogle, E. S.; Pople, J. A. *Gaussian 98*, revision A.7; Gaussian, Inc.: Pittsburgh, PA, 1998.

(32) Magalhaes, A. L.; Soares Pinto, A. S. *Theor. Chem. Acc.* **2003**, *110*, 70.

(33) Jarvis, G. K.; Weitzel, K. M.; Malow, M.; Baer, T.; Song, Y.; Ng, C. Y. *Phys. Chem. Chem. Phys.* **1999**, *1*, 5259.

(34) Weitzel, K. M.; Malow, M.; Jarvis, G. K.; Baer, T.; Song, Y.; Ng, C. Y. *J. Chem. Phys.* **1999**, *111*, 8267.

(35) Weitzel, K. M.; Jarvis, G. K.; Malow, M.; Baer, T.; Song, Y.; Ng, C. Y. *Phys. Rev. Lett.* **2001**, *86*, 3526.

(36) Blush, J. A.; Chen, P.; Wiedmann, R. T.; White, M. G. *J. Chem. Phys.* **1993**, *98*, 3557.

(37) Hunter, E. P. L.; Lias, S. G. *J. Phys. Chem. Ref. Data* **1998**, *27*, 413.

(38) Murad, E.; Inghram, M. G. *J. Chem. Phys.* **1964**, *41*, 404.

(39) [a]Frequencies calculated at the B3LYP/6-311++G** level of theory.